Paracrine Wnt/β-catenin signaling mediates proliferation of undifferentiated spermatogonia in the adult mouse testis

Hinako M. Takase[a,b,c] and Roeland Nusse[a,b,1]

[a]Department of Developmental Biology, Stanford University, Stanford, CA 94305; [b]Howard Hughes Medical Institute, Stanford University, Stanford, CA 94305; and [c]Department of Experimental Animal Model for Human Disease, Tokyo Medical and Dental University, Bunkyo-ku, Tokyo 113-8510, Japan

Contributed by Roeland Nusse, January 28, 2016 (sent for review October 20, 2015; reviewed by Thomas Carroll and Shosei Yoshida)

Spermatogonial stem cells (SSCs) fuel the production of male germ cells but the mechanisms behind SSC self-renewal, proliferation, and differentiation are still poorly understood. Using the Wnt target gene *Axin2* and genetic lineage-tracing experiments, we found that undifferentiated spermatogonia, comprising SSCs and transit amplifying progenitor cells, respond to Wnt/β-catenin signals. Genetic elimination of β-catenin indicates that Wnt/β-catenin signaling promotes the proliferation of these cells. Signaling is likely initiated by Wnt6, which is uniquely expressed by neighboring Sertoli cells, the only somatic cells in the seminiferous tubule that support germ cells and act as a niche for SSCs. Therefore, unlike other stem cell systems where Wnt/β-catenin signaling is implicated in self-renewal, the Wnt pathway in the testis specifically contributes to the proliferation of SSCs and progenitor cells.

spermatogonia | stem cells | Wnt | testis

By continuously self-renewing, proliferating, and differentiating, spermatogonial stem cells (SSCs) produce millions of sperm cells each day throughout the reproductive period in mammals (1). Despite the importance of SSCs, the molecular mechanisms of their regulation remain largely unknown. Although infertility is a major reproductive health problem, the cause of human male infertility is often obscure (2, 3). It is important, therefore, to understand the underlying molecular mechanisms that govern SSC behavior during homeostasis.

Spermatogenesis takes place in the seminiferous tubules. Sertoli cells, the only somatic cell population within seminiferous tubules, support all germ cells, including SSCs. Spermatogonia reside on the basement membrane and, as the cells differentiate, they move toward the lumen. Thus far, the exact identity of SSCs has been uncertain; they are thought to be contained within a small population of cells known as "undifferentiated spermatogonia" (4).

Undifferentiated spermatogonia are subdivided into spermatogonial types A_{single} (A_s; isolated single cells), A_{paired} (A_{pr}; chains of two cells) and $A_{aligned}$ (A_{al}; chains of 4, 8, or 16 cells) based on their morphological characteristics. In an ordered process, undifferentiated spermatogonia undergo maturation, followed by meiosis, to give rise to spermatozoa. In the 1970s, the so-called "A_s model" was proposed to explain the identity and behavior of SSCs based on ^{3}[H] thymidine incorporation assays (5). This model postulates that stem cell function is restricted to A_s spermatogonia that can produce A_{pr} and A_{al} spermatogonia as progenitor cells (4). On the other hand, recent studies have suggested the possibility of contributions of A_{pr} and A_{al} spermatogonia, as well as A_s, cells to the SSC pool, based on live imaging and mathematical modeling (6, 7). In those studies, the investigators observed the fragmentation of A_{pr} and A_{al} cells to provide A_s spermatogonia, and proposed that GFRα1$^+$ spermatogonia form a single SSC pool that constantly interchanges between A_s and syncytial states. These studies raised the possibility that SSCs behave dynamically and flexibly. Taken together, there is agreement that A_s, A_{pr}, and A_{al} undifferentiated spermatogonia contain SSCs; however, additional markers and lineage-tracing experiments are needed to clarify the relationships between the different cell types.

The fates of tissue stem cells are usually regulated by a specialized microenvironment, referred to as a niche. In the testis, Sertoli cells are considered a key somatic cell population that functions as a niche by providing growth factors, such as GDNF, which is a critical factor for the self-renewal and maintenance of SSCs (8). Although considerable effort has been invested into understanding the basic molecular mechanisms underlying SSC regulation, there are still microenvironmental cell–cell interactions that remain to be elucidated. For example, the mechanism by which cell–cell signaling controls the rate of SSC proliferation is not well understood.

Wnt signaling is a highly conserved cell-to-cell communication mechanism, consisting of a canonical and noncanonical branch. Canonical Wnt signaling is also referred to as the Wnt/β-catenin pathway and is often implicated as a stem cell self-renewal mechanism (9). During development, Wnt/β-catenin signaling is required for the specification of primordial germ cells and the proper development of the male fetal reproductive tract (10–12). In contrast, limited information is available regarding the importance of Wnt signaling in the postnatal testis. Previous in vitro studies have suggested a possible contribution of the Wnt pathway to SSC regulation; for example, Yeh et al. reported that Wnt5a, a ligand for the noncanonical Wnt pathway, supports SSC survival by suppressing apoptosis (13). These authors also

Significance

Spermatogonial stem cells are unique among adult tissue stem cells in their role in transmitting genetic information to the next generation. Germ-line stem cells in *Caenorhabditis elegans* and *Drosophila* are well studied because of their relatively simple organization with a clear anatomical niche, but the regulatory mechanisms behind mammalian spermatogonial stem cells are less well understood. In this report, we demonstrate that the proliferation of undifferentiated spermatogonia, including spermatogonial stem cells, is controlled by Wnt/β-catenin signaling. Wnts are secreted by Sertoli cells, which thereby act as a niche. To our knowledge, this work proves, for the first time, that Wnt/β-catenin signaling is involved in spermatogonial stem/progenitor cell regulation in vivo, and also uncovers its mode of action.

Author contributions: H.M.T. and R.N. designed research; H.M.T. performed research; H.M.T. contributed new reagents/analytic tools; H.M.T. and R.N. analyzed data; and H.M.T. and R.N. wrote the paper.

Reviewers: T.C., University of Texas Southwestern Medical Center; and S.Y., National Institute for Basic Biology.

The authors declare no conflict of interest.

Freely available online through the PNAS open access option.

[1]To whom correspondence should be addressed. Email: rnusse@stanford.edu.

This article contains supporting information online at www.pnas.org/lookup/suppl/doi:10.1073/pnas.1601461113/-/DCSupplemental.

showed that Wnt3a promotes proliferation of a subset of cultured cells via Wnt/β-catenin pathway, and proposed that these Wnt-responsive cells possess the character of progenitors rather than SSCs (14). Another study reported that Wnt3a and Wnt10b proteins can promote proliferation of a mouse SSC line, C18-4 (15).

In this study, we investigated the function of Wnt/β-catenin signaling pathway in vivo, by taking advantage of genetic lineage tracing using Axin2 as a marker of Wnt/β-catenin pathway-responsive cells (16, 17). Our study revealed that undifferentiated spermatogonia expressing Axin2 contain SSCs. Our data also suggest that undifferentiated spermatogonia are supported by Wnt6 ligand from Sertoli cells. Thus, under physiological conditions, paracrine Wnt/β-catenin signaling controls the proliferation of undifferentiated spermatogonia.

Results

Axin2 Marks Undifferentiated Spermatogonia. Axin2 expression reflects Wnt/β-catenin signaling activation and is a useful marker for functional stem cells in a variety of tissues (17–21). In Axin2-LacZ reporter mice, we observed LacZ signals in a subset of the cells near the basement membrane, but not in postmeiotic germ cells residing in the adluminal compartment of the seminiferous epithelium (Fig. 1 *A* and *B*). To identify Axin2$^+$ cells, we performed immunostaining on LacZ-stained sections with markers for undifferentiated spermatogonia, glial cell line-derived neurotrophic factor family receptor-α1 (GFRα1) and promyelocytic leukemia zinc-finger (PLZF). GFRα1 primarily marks A_s and A_{pr} as a marker for SSC-enriched subpopulations of undifferentiated spermatogonia (6, 22, 23), whereas PLZF marks A_s, A_{pr}, and A_{al} cells as a pan-undifferentiated spermatogonia marker (24, 25). LacZ signals were present together with GFRα1 and PLZF immunoreactivity, indicating that undifferentiated spermatogonia are Wnt-responsive cells (Fig. 1 *C* and *D*). Stereological analysis indicated that 77.5% and 53.5% of GFRα1 and PLZF$^+$ cells, respectively, were LacZ$^+$ (Fig. 1*E*).

To label and follow the fate of Axin2$^+$ cells, we crossed Axin2^{CreERT2} mice with the Rosa26^{mTmG} reporter strain for inducible genetic lineage tracing (17, 26). In Axin2$^{CreERT2/+}$;Rosa26$^{mTmG/+}$ mice, a subpopulation of Axin2$^+$ cells are stochastically labeled with membrane GFP upon tamoxifen administration (Fig. 2*A*). By whole-mount imaging assays on pulse-labeled Axin2$^{CreERT2/+}$;Rosa26$^{mTmG/+}$ mice [2-d traced from postnatal (P) day 56], we confirmed the identities of the initially labeled cells. Labeled GFP$^+$ cells were found across all subpopulations of undifferentiated spermatogonia (i.e., A_s, A_{pr}, and A_{al} cells), with A_{al-4} and A_{al-8} spermatogonia having the highest labeling frequency (Fig. 2*B*). Immunofluorescence revealed that GFP$^+$ cells contain both a GFRα1$^+$ and GFRα1$^-$ populations (Fig. 2*C*). The results showed that 12.8% of all GFP$^+$ cells are positive for GFRα1 (Fig. 2*F*), with the highest percentage of GFRα1$^+$ cells in the GFP$^+$ A_s subpopulation (Fig. 2*G*). On the other hand, 95.5% of labeled GFP$^+$ cells were PLZF$^+$ undifferentiated spermatogonia, defining them as A_s, A_{pr}, and A_{al} populations (Fig. 2 *D* and *H*). The remaining 4.5% of labeled GFP$^+$ cells were PLZF$^-$ and mostly belonged to the subpopulation of A_{al} spermatogonia chains of more than 16 cells (Fig. 2*I*). In contrast, GFP$^+$ cells were negative for cKit, which marks differentiating spermatogonia (Fig. 2*E*). Thus, the immunostaining pattern of stage-specific germ cell markers indicates that pulse-labeled Axin2$^+$ cells are contained within the undifferentiated spermatogonia population. Meanwhile, we found a low labeling efficiency in the testis of Axin2$^{CreERT2/+}$;Rosa26$^{mTmG/+}$ mice (Fig. 2*J*): only 0.6% of GFRα1$^+$ cells and 2.5% of PLZF$^+$ cells were marked after single dose of tamoxifen injection. This result indicates that there is a slight difference when labeling cell populations with Axin2-LacZ and Axin2$^{CreERT2/+}$;Rosa26$^{mTmG/+}$; that is, Axin2-LacZ marks a large fraction of GFRα1$^+$ cells whereas Axin2$^{CreERT2/+}$;Rosa26$^{mTmG/+}$ predominantly labels PLZF$^+$ cells.

Axin2$^+$ Cells Contain SSCs. To study the contribution of pulse-labeled Wnt-responsive spermatogonia to spermatogenesis, we executed a series of lineage-tracing experiments. We administered tamoxifen to Axin2$^{CreERT2/+}$;Rosa26$^{mTmG/+}$ mice at P56 and analyzed the testis 2 d, 1 wk, 2 wk, 4 wk, 12 wk, or 6 mo thereafter (Fig. 3*A*). Images of tdTomato are included in Fig. 3*B* to

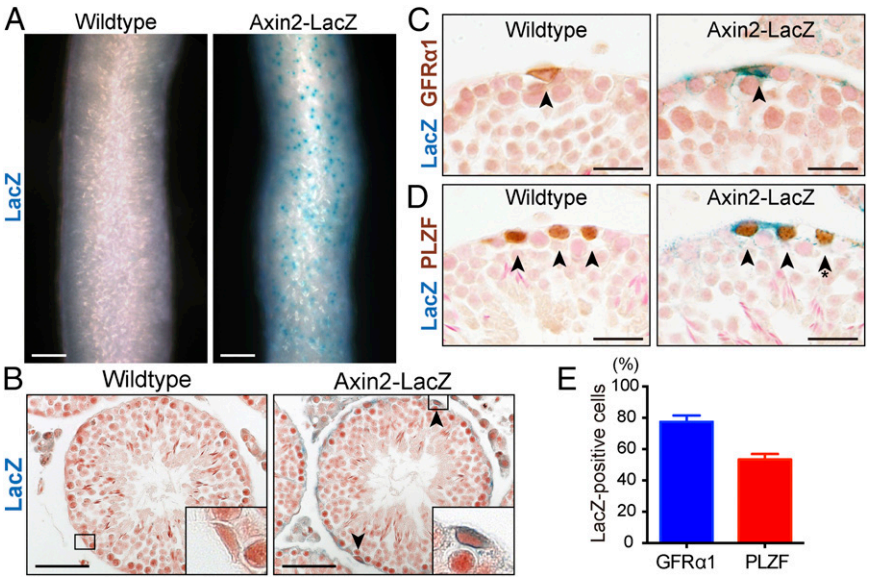

Fig. 1. Wnt/β-catenin responsive cells in the adult mouse testis are undifferentiated spermatogonia. Seminiferous tubules from 2-mo-old (P56) wild-type and Axin2-LacZ mice. (*A*) Dark-field images of X-gal–stained whole-mount seminiferous tubules. (Scale bar, 50 μm.) (*B*) Histological X-gal–stained sections counterstained with Nuclear Fast Red. Boxed areas are magnified in insets. (Magnification: 3.9×.) Arrowheads indicate Axin2-LacZ$^+$ cells. (Scale bars, 50 μm.) (*C*) Immunostaining with anti-GFRα1 (brown) antibody on X-gal–stained tissue sections. Arrowheads indicate GFRα1$^+$ cells. (Scale bars, 20 μm.) (*D*) Immunostaining with anti-PLZF (brown) antibody on X-gal–stained tissue sections. Arrowheads indicate PLZF$^+$ cells. The asterisk indicates a LacZ$^-$ cell. (Scale bars, 20 μm.) (*E*) Percentages of LacZ$^+$ cells within GFRα1 or PLZF$^+$ population calculated by a stereological method. $n = 3$ mice per group. Error bars represent SEM.

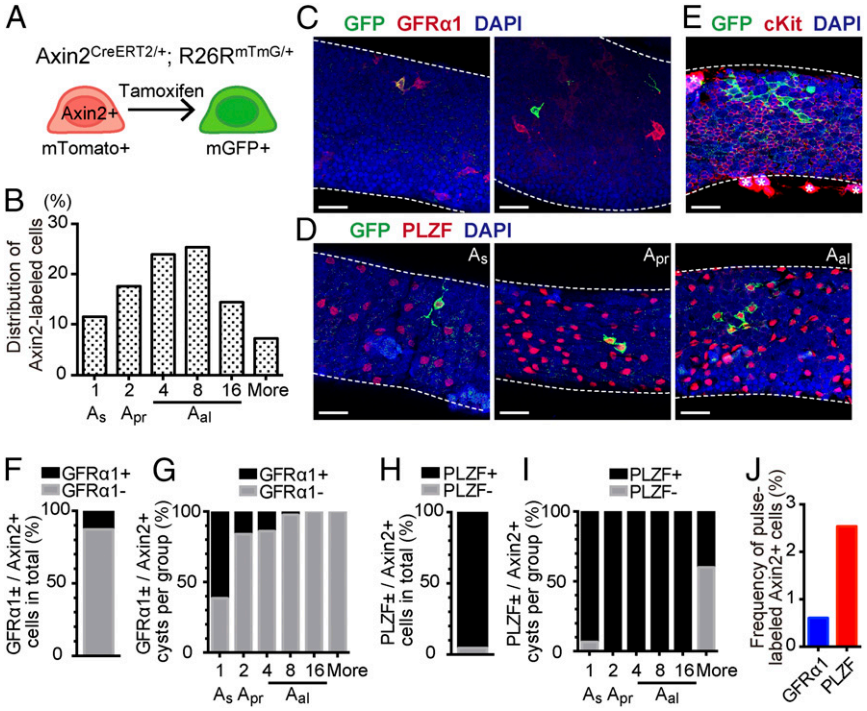

Fig. 2. Axin2^{CreERT2} marks undifferentiated spermatogonia upon pulse-labeling. (*A*) Schematic view of genetic cell labeling using Axin2$^{CreERT2/+}$;Rosa26$^{mTmG/+}$ mice. Tamoxifen administration induces GFP expression in a subset of Axin2-expressing cells and their progeny. (*B*) Frequency of undifferentiated spermatogonia populations classified by cellular morphology 2 d after tamoxifen pulse. The *x* axis indicates the number of chained cells. A total of 347 pulse-labeled cysts from four animals were counted. (*C*) Whole-mount images of GFP (green) and GFRα1 (red) immunostaining and DAPI (blue) staining of Axin2$^{CreERT2/+}$;Rosa26$^{mTmG/+}$ seminiferous tubules traced for 2 d. (*Left*) GFRα^{+} pulselabeled cells; (*Right*) GFRα^{-} pulse-labeled cells. (Scale bars, 50 μm.) (*D*) Whole-mount images of GFP (green) and PLZF (red) immunostaining and DAPI (blue) staining of Axin2$^{CreERT2/+}$;Rosa26$^{mTmG/+}$ seminiferous tubules traced for 2 d. Subpopulations of labeled undifferentiated spermatogonia were evaluated by the number of chained cells. (Scale bars, 50 μm.) (*E*) Whole-mount images of GFP (green) and cKit (red) immunostaining and DAPI (blue) staining of Axin2$^{CreERT2/+}$;Rosa26$^{mTmG/+}$ seminiferous tubules traced for 2 d. Asterisks denote Leydig cells. (Scale bars, 50 μm.) (*F*) Frequency of GFRα1^{+} or GFRα1^{-} cells in total pulse-labeled cysts of undifferentiated spermatogonia from Axin2$^{CreERT2/+}$;Rosa26$^{mTmG/+}$ mice. A total of 252 pulse-labeled cysts and 45.5 cm of seminiferous tubules from four animals were analyzed. (*G*) Frequency of GFRα1^{+} or GFRα1^{-} cells within each pulse-labeled spermatogonia clusters. (*H*) Frequency of PLZF^{+} or PLZF^{-} cells in total pulse-labeled cysts of undifferentiated spermatogonia. A total of 195 pulse-labeled cysts and 37.9 cm of seminiferous tubules from four animals were analyzed. (*I*) Frequency of PLZF^{+} or PLZF^{-} cells within each pulse-labeled spermatogonia clusters. (*J*) Percentages of GFP-labeled cells within GFRα1^{+} or PLZF^{+} cells. n = 10,311 (GFRα1) and n = 42,034 (PLZF) cells, four animals for each were analyzed.

outline seminiferous tubules, as basement membranes are well visible by their strong fluorescence intensity among ubiquitous tdTomato expression (26). In a cross-sectional view of a 2-d traced testis, we observed labeled GFP^{+} undifferentiated spermatogonia near the basement membrane, as expected (Fig. 3*B*), whereas occasionally somatic cell types, such as peritubular myoid cells, blood vessel, and Sertoli cells were labeled. However, differentiated germ cell types, such as differentiating spermatogonia, spermatocytes, spermatids, and spermatozoa were not labeled. Within 2 wk of the initial labeling, the offspring of labeled germ cells were found as clusters containing differentiating spermatogonia based on morphology (27) (Fig. 3*B*). Upon tracing for 4 wk, we detected GFP^{+} clones harboring all stages of spermatogenic cells (Fig. 3*B*). GFP^{+} clones increased in size over time and persisted for at least 6 mo (Fig. 3*B*), a period well beyond the normal duration of spermatogenesis, which spans 35–40 d from the earliest undifferentiated spermatogonia to mature spermatozoa in mice (28, 29).

Thus, this lineage-tracing experiment demonstrates that Axin2-labeled cells and their progeny persist for numerous rounds of spermatozoa turnover and we reasoned that the GFP^{+} clones would contain undifferentiated spermatogonia to sustain clonal expansion. To this end, we immunostained 12-wk–traced Axin2$^{CreERT2/+}$;Rosa26$^{mTmG/+}$ mice with anti-GFRα1 antibody. Multiple GFRα1^{+} cells were found within GFP^{+} clones after long-term tracing (Fig. 3*C*), suggesting that labeled Axin2^{+} cells are capable of generating more undifferentiated spermatogonia. We concluded that the Wnt-responding population include SSCs that meet the definition of stem cells: able to give rise to all of the differentiating germ cell types and self-renewing over the long term.

Despite these findings, the extent to which GFP^{+} spermatogonia can self-renew as SSCs remained unclear, as did their differentiation ability. To determine the number of GFP^{+} cells that remain as undifferentiated spermatogonia, GFP^{+} undifferentiated spermatogonia were counted according to the number of chained cells at different time points after tamoxifen administration. The number of cysts per testis was calculated according to a previously reported study (30). GFP^{+} A_s, A_{pr}, and A_{al} were observed 2 d after tamoxifen injection with a peak in $A_{al\text{-}4}$ and $A_{al\text{-}8}$ spermatogonia, as expected from the results shown in Fig. 2*B* (Fig. 3*D*). Within 1 wk, longer chains of A_{al} spermatogonia were shifted to more differentiated spermatogonia, whereas decreased numbers of GFP^{+} undifferentiated spermatogonia were detected after 2 wk (Fig. 3*D*). If SSCs were marked specifically, the total number of shorter chains of undifferentiated spermatogonia, such as A_s, A_{pr}, and presumably $A_{al\text{-}4}$, should not change over time (31). Thus, our result suggests that Axin2$^{CreERT2/+}$;Rosa26$^{mTmG/+}$ mostly marks progenitor-like cells within undifferentiated spermatogonia, whereas a few SSCs are also labeled.

The tamoxifen dose used for Axin2$^{CreERT2/+}$;Rosa26$^{mTmG/+}$ mice during lineage-tracing experiments usually gave rise to

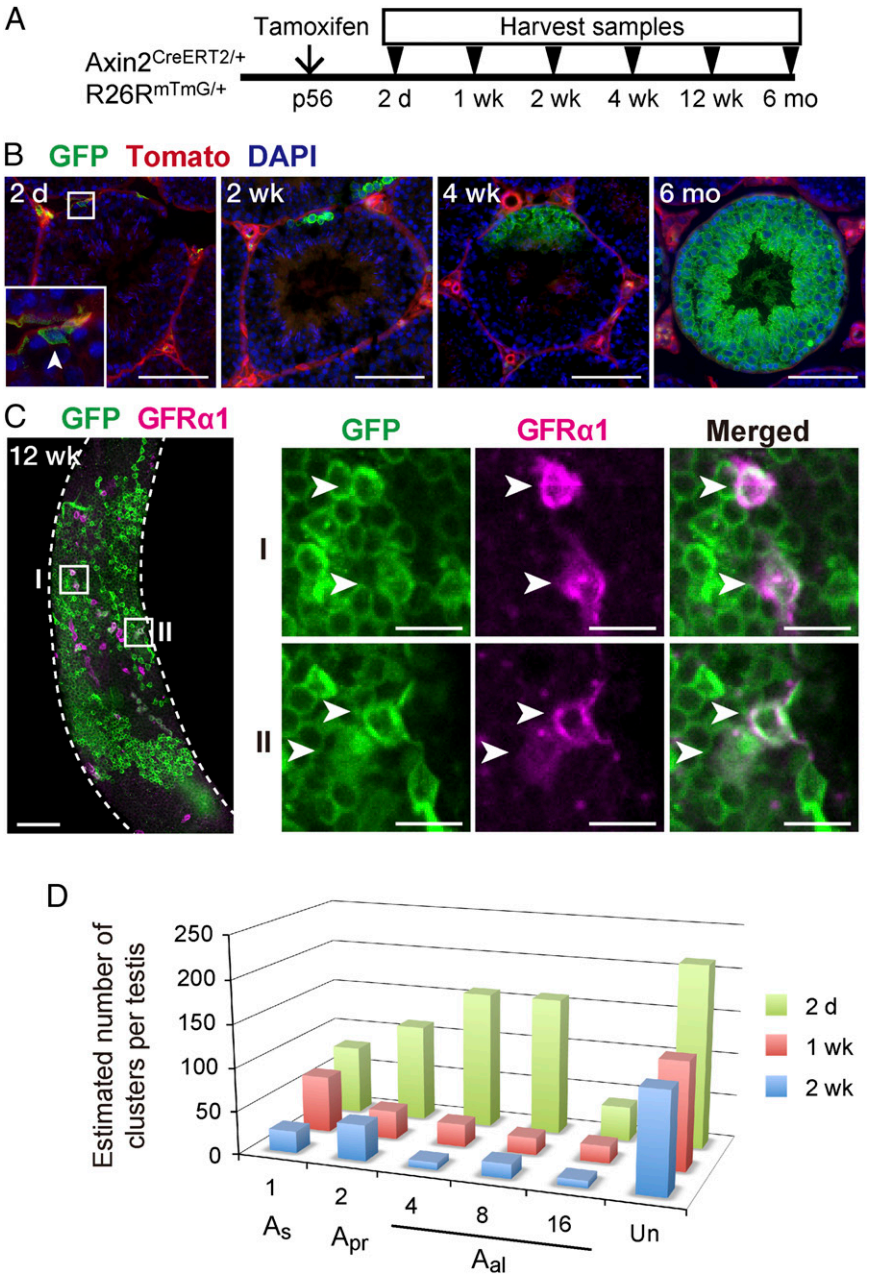

Fig. 3. Wnt/β-catenin responsive spermatogonial stem cells contribute to normal spermatogenesis. (*A*) Experimental schedule used in *B–D* for lineage tracing experiments. (*B*) Cross-sectional images of GFP (green) immunostaining, tdTomato (red) and DAPI (blue) of Axin2$^{CreERT2/+}$;Rosa26$^{mTmG/+}$ seminiferous tubules traced for 2 d, 2 wk, 4 wk, or 6 mo from P56. Arrowhead indicates pulse-labeled spermatogonia. (Scale bars, 100 μm.) (*C*) Whole-mount immunostaining of Axin2$^{CreERT2/+}$;Rosa26$^{mTmG/+}$ seminiferous tubules for GFP (green) and GFRα1 (magenta) 12 wk after pulse labeling. The outlines of seminiferous tubules are indicated by dashed lines. Boxed areas (I and II) are magnified, *Right*. Arrowheads indicate GFP-GFRα1 double-positive cells. [Scale bars, 100 μm (*Left*) and 20 μm (*Right*).] (*D*) Estimated numbers of the labeled undifferentiated spermatogonia populations per testis classified by cellular morphology 2 d, 1 wk, or 2 wk after tamoxifen injection. Un, unclassified undifferentiated spermatogonia in which cell numbers were not determined. A total of 115 (2 d), 44 (1 wk), and 26 (2 wk) cysts and 63.3 (2 d), 64.1 (1 wk), and 50.6 cm (2 wk) of seminiferous tubules from three animals for each time point were analyzed.

sporadic labeling of single cells in pulse-labeled testis (Fig. 2 *C* and *D*). Furthermore, individual GFP$^+$ cell clones were separated by large stretches of unlabeled epithelium after tracing, suggesting that they were clonal off-spring cells of a single recombination event (Fig. 3*C*). To distinguish precisely between labeled cells and their descendants from adjacent cells, we took advantage of a multicolor lineage tracing method using "Rainbow (Rosa26^{rbw})" mice (32). Rosa26^{rbw} is a multicolor Cre-dependent marker system that allows stochastic expression of one of three fluorescent proteins (mCerulean, mOrange, or mCherry) following Cre-mediated recombination (Fig. 4*A*). We injected Axin2$^{CreERT2/+}$;Rosa26$^{rbw/+}$ mice with a single dose of tamoxifen at P56. Axin2$^{CreERT2/+}$;Rosa26$^{rbw/+}$ mice were killed and analyzed after 1 wk, 4 wk, 12 wk, and 6 mo (Fig. 4*B*). In confocal images of cross-sections of Axin2$^{CreERT2/+}$;Rosa26$^{rbw/+}$ testis, colored spermatogonia were first identified 7 d postlabeling and were found scattered throughout the basal layer of seminiferous tubules (Fig. 4*C*). At 4 wk, we observed single-color clones adjacent to each other, reflecting a heterogeneous labeling pattern and the expansion of individual clones (Fig. 4*C*). At later time points, we

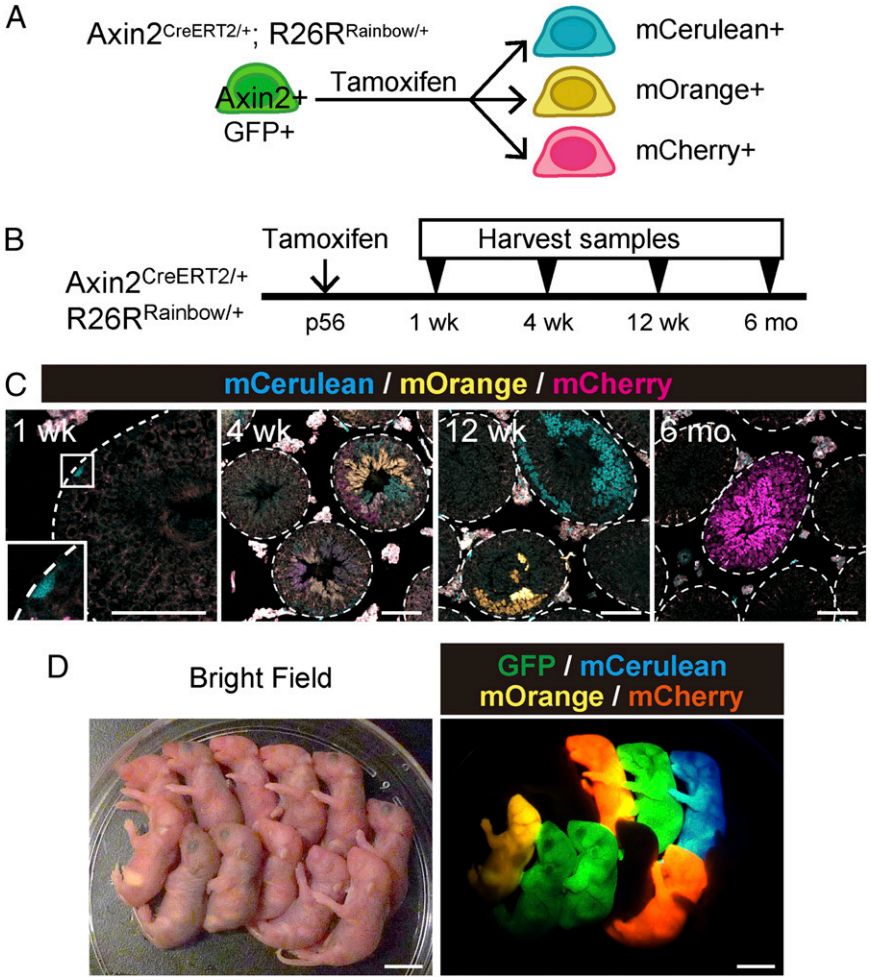

Fig. 4. Multicolor lineage tracing reveals clonal expansion of labeled Axin2^{+} cells. (*A*) Schematic view of genetic cell labeling experiments using Axin2$^{CreERT2/+}$;Rosa26$^{rbw/+}$ mice. Tamoxifen administration randomly induces expression of one of three fluorescent proteins, mCerulean, mOrange, or mCherry, in a subset of Axin2-expressing cells and their progeny. (*B*) Experimental schedule used in *C* for multicolor lineage tracing study. (*C*) Cross-sectional images of Axin2$^{CreERT2/+}$;Rosa26$^{rbw/+}$ seminiferous tubules traced for 1 wk, 4 wk, 12 wk, or 6 mo from P56. Boxed area is magnified in *Inset*. (Magnification: 2.5×.) The outlines of seminiferous tubules are indicated by dashed lines. (Scale bars, 80 μm.) (*D*) Newborn offspring from intercrosses of wild-type female and 6-wk–traced Axin2$^{CreERT2/+}$;Rosa26$^{rbw/+}$ male. (*Left*) Bright field; (*Right*) fluorescence images taken with filter sets for GFP, mCerulean, mOrange, and mCherry and subsequently overlayed. (Scale bars, 1 cm.)

found a continuing expansion of average clone size until the cross-sections of seminiferous tubules became either fully labeled with one color or fully unlabeled (Fig. 4*C*). These results are consistent with a neutral competition model in which tissue stem cells are routinely lost and replaced in a stochastic manner, as previously demonstrated by the use of specific Cre lines of GFRα1, Ngn3, and Bmi1 in the testis (6, 31, 33, 34).

Next, we sought to prove that the Wnt-responsive SSC population actually produces functional, mature spermatozoa. Axin2$^{CreERT2/+}$;Rosa26$^{rbw/+}$ males that received a single high dose of tamoxifen (10-mg/20-g body weight) were traced for 6–12 wk and then mated with wild-type females. We obtained pups of all three colors within a single litter (Fig. 4*D*). Hence, this result further demonstrates the presence of long-lived Wnt-responsive SSCs in the mouse testis, which give rise to mature spermatozoa with normal reproductive potential.

Wnt/β-Catenin Signaling Is Required for Proliferation of Undifferentiated Spermatogonia in Vivo. To test a functional requirement for Wnt/β-catenin signaling in Axin2^{+} undifferentiated spermatogonia, we undertook a loss-of-function approach by conditionally deleting the β-catenin gene in Axin2-expressing cells upon tamoxifen injection (35). β-Catenin is an essential component of canonical Wnt/β-catenin signaling, acting as an intracellular signal transducer (9). Control Axin2$^{CreERT2/+}$;β-catenin$^{Δex2\text{-}6\text{-}fl/+}$ mice and mutant Axin2$^{CreERT2/+}$;β-catenin$^{Δex2\text{-}6\text{-}fl/del}$ mice received three doses of tamoxifen administration (3-mg/20-g body weight) at P56–P60 and were analyzed 5 wk after the treatment (Fig. 5*A*). Under these conditions, no significant loss of body weight was observed in β-catenin mutant mice (Fig. S1*A*). β-Catenin expression in the testes of mutant mice was reduced compared with that in the controls as shown by immunostaining, confirming the deletion of β-catenin in the mutant testis (Fig. S1*B*). Testis weights of β-catenin mutant mice were significantly reduced compared with those of littermate controls, with an average reduction of 25% (Fig. 5 *B* and *C*). Histological analysis indicated that the β-catenin mutant testes show a loss of germ-cell phenotype (Fig. 5*D*). Specifically, the seminiferous tubules of β-catenin mutants were reduced in diameter and lacked the normal organization of the seminiferous epithelium. Within a single section of the testis, we observed seminiferous tubules with very severe to relatively mild phenotypes (Fig. S1 *D* and *E*), presumably because of the mosaic deletion of β-catenin within the Axin2^{+} population.

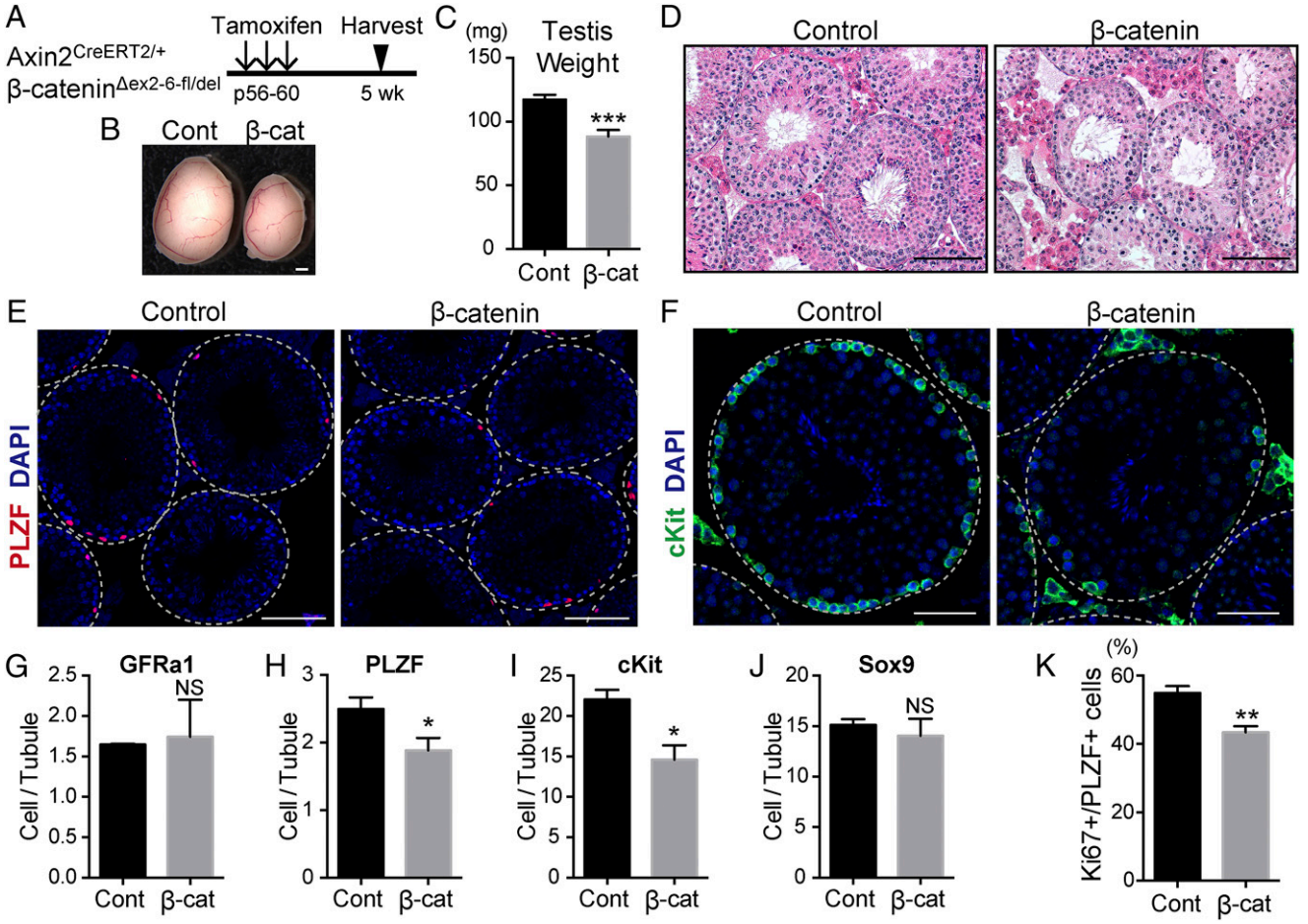

Fig. 5. Deletion of β-catenin results in reduced proliferation of undifferentiated spermatogonia. (*A*) Experimental schedule used in *B–K* for conditional β-catenin knockout experiments. (*B*) Gross morphology of testes from control Axin2$^{CreERT2/+}$;β-catenin$^{\Delta ex2\text{-}6\text{-}fl/+}$ (Cont) and mutant Axin2$^{CreERT2/+}$;β-catenin$^{\Delta ex2\text{-}6\text{-}fl/del}$ (β-cat) littermates. (Scale bar, 1 mm.) (*C*) Average testis weight of control (Cont, $n = 10$) and β-catenin mutant (β-cat, $n = 11$) mice. Error bars represent SEM. ***Statistical difference of $P < 0.001$. (*D*) H&E staining of testes from control and β-catenin mutant mice. (Scale bars, 100 μm.) (*E*) Cross-sectional images of PLZF (red) immunostaining and DAPI (blue) staining of control and β-catenin mutant testis. The outlines of seminiferous tubules are indicated by dashed lines. (Scale bars, 100 μm.) (*F*) Cross-sectional images cKit (green) immunostaining and DAPI (blue) staining of control and β-catenin mutant seminiferous tubules at stage VII-VIII. (Scale bars, 50 μm.) (*G–J*) The number of GFRα1$^+$ (*G*), PLZF$^+$ (*H*), cKit$^+$ (*I*), or Sox9$^+$ (*J*) cells per seminiferous tubule in sections from control (Cont) and β-catenin mutant (β-cat) mice. More than 150 tubules from three independent tiled confocal images of an entire testis cross section were counted ($n = 3$). Error bars represent SEM. *Statistical difference of $P < 0.05$. NS, not significant. (*K*) The percentage of Ki67$^+$ cells in total PLZF$^+$ cells of control (Cont) and β-catenin mutant (β-cat) testis. More than 150 tubules from six independent tiled confocal images of an entire testis cross-section were counted ($n = 3$). Error bars represent SEM. **Statistical difference of $P < 0.01$.

To determine the nature of the germ cells depleted in β-catenin mutant testes, we performed immunostaining with markers for undifferentiated spermatogonia. The numbers of GFRα1$^+$ undifferentiated spermatogonia in β-catenin mutant testes and in control testes were similar, suggesting that the maintenance of SSCs was not affected in this experiment (Fig. 5*G*). However, the number of PLZF$^+$ undifferentiated spermatogonia per seminiferous tubule cross section was significantly lower in mutants (Fig. 5 *E* and *H*). Moreover, double-immunostaining using PLZF and a proliferation marker, Ki67, indicated that PLZF$^+$ undifferentiated spermatogonia were less proliferative in β-catenin mutant testis tissue compared with the control (Fig. 5*K*). Similarly, there were fewer cKit$^+$ differentiating spermatogonial cells and the remaining cells were disorganized in the β-catenin mutants (Fig. 5 *F* and *I* and Fig. S1*D*). On the other hand, the number of Sox9$^+$ Sertoli cell was not affected by β-catenin deletion (Fig. 5*J*). Because we rarely observed activated caspase 3$^+$ apoptotic germ cells in β-catenin mutants or controls (Fig. S1*C*), these data indicate that the testicular atrophy of the β-catenin mutant mice was caused by suppression of proliferation in undifferentiated spermatogonia, resulting in subsequent loss of differentiating spermatogonia and other germ-cell types.

Sertoli Cells Secrete Wnt6 as a Paracrine Signal for Undifferentiated Spermatogonia. For a more complete understanding of how Wnt signaling regulates the proliferation of undifferentiated spermatogonia, we wanted to identify the cells that produce Wnt ligands by RNA in situ hybridization for the 19 Wnt ligands (Fig. S2). From this survey, we found *Wnt6* to be specifically expressed in the Sertoli cells, particularly in the basal compartment where undifferentiated spermatogonia reside (Fig. 6*A*). We confirmed this by double-labeling RNA in situ hybridization using *Sox9* as a marker for Sertoli cells in the testis (Fig. 6*B*). Wnt ligands are secreted glycoproteins that predominantly work over short ranges to control cell behavior locally (9). In addition, the seminiferous epithelium is divided into basal and adluminal compartments by continuous tight junctions (blood–testis barrier) of Sertoli cells, and forms one of the tightest blood–tissue barriers in the mammalian body, restricting passage of molecules between two compartments (4). Therefore, from this analysis of expression sites, we

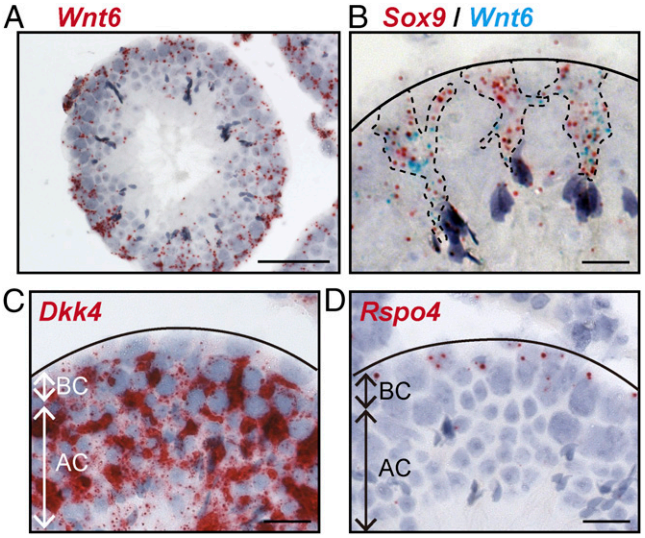

Fig. 6. Wnt6 is a niche signal for undifferentiated spermatogonia produced by Sertoli cells. (*A*) In situ hybridization of *Wnt6* (red) on testis sections from adult wild-type mice (P56). (Scale bar, 50 μm.) (*B*) Double-labeling RNA in situ hybridization for expression of *Sox9* (red, a Sertoli cell marker) and *Wnt6* (turquoise). Dashed lines indicate the estimated outlines of Sertoli cells. Solid line indicates the approximate location of the basal layer of seminiferous tubule. (Scale bar, 10 μm.) (*C* and *D*) In situ hybridization of *Dkk4* (red, *C*) or *Rspo4* (red, *D*) on testis sections. AC, adluminal compartment; BC, basal compartment. Solid line indicates the approximate location of the basal layer of seminiferous tubule. (Scale bars, 10 μm.)

considered Wnt6 to be the family member most likely to act on undifferentiated spermatogonia. However, the Wnt ligand expression pattern alone does not adequately explain how undifferentiated spermatogonia can be activated selectively, because Sertoli cells are large cells than span both the basal and adluminal compartments and, therefore, could conceivably secrete Wnt ligands in both the compartments. We also determined the expression patterns of Wnt inhibitors and activators by RNA in situ hybridization, because these contribute to the precise regulation of Wnt/β-catenin signaling (36). We found that one Wnt inhibitor, *Dkk4*, was highly expressed in the adluminal compartment, but not in the basal compartment (Fig. 6*C*). In addition, the expression of *Rspo4*, an activator of Wnt/β-catenin signaling, was localized to the basal compartment (Fig. 6*D*). These data support the notion that Wnt6 stimulates canonical Wnt/β-catenin signaling in undifferentiated spermatogonia, aided by the basal compartment-specific Rspo4 expression, whereas Dkk4 blocks activation of Wnt/β-catenin signaling in the adluminal compartment where meiotic spermatocytes, spermatids, and spermatozoa reside.

Intriguingly, other Wnts were expressed in the seminiferous tubules, in highly specific expression patterns (Fig. S2). For example, we detected the expression of *Wnt3* in round spermatids and elongating spermatids, *Wnt3a* in round spermatids, *Wnt5a* in Leydig cells and peritubular myoid cells, *Wnt7a* in pachytene spermatocytes and round spermatids, and *Wnt8b* in round spermatids. These gene-expression patterns are compatible with previously published transcriptional profiling data (37–39).

Discussion

This study demonstrates that Wnt/β-catenin signaling is a key regulator of the proliferation of undifferentiated spermatogonia. In this scenario, undifferentiated spermatogonia, including SSCs, receive Wnt6 secreted by Sertoli cells, leading to activation of Wnt/β-catenin signaling and subsequent expression of Wnt target genes, such as *Axin2* (Fig. 7). Although in vitro experiments have indicated that Wnt3a and Wnt5a support SSC activity (13–15), we found that in vivo Sertoli cells, known to act as a niche for undifferentiated spermatogonia, specifically produce Wnt6 and none of the other Wnts (Fig. 6*B*). Our findings contribute to the molecular understanding of spermatogonia regulation by its niche, which may provide us with new insight about the etiology of male infertility.

As in previous tracing experiments including stem cell lineages, we used the Wnt target gene *Axin2* as a marker for Wnt-responding cells (21, 40, 41). Although the activation of Wnt/β-catenin signaling in round spermatids has been reported using the BAT-gal and the TCF/Lef-LacZ mouse reporter lines (13, 42), Wnt reporter activity in undifferentiated spermatogonia has not been described previously. Our data clearly indicate that GFRa1$^+$ and PLZF$^+$ undifferentiated spermatogonia are Wnt-responsive as judged by Axin2-LacZ expression (Fig. 1 *C* and *D*). The discordance between Wnt-responsive populations observed in previous studies and in ours may be caused by differences between mouse lines, as seen in other tissues as well (43), and also raises the possibility that Wnt/β-catenin signaling plays a role at multiple stages during spermatogenesis.

It has been proposed that undifferentiated spermatogonia constitute a heterogeneous population consisting of two groups with different gene expression and stem cell potentials: an SSC-enriched GFRα1$^+$/Nanos2$^+$ population and a progenitor-like Ngn3$^+$/Nanos3$^+$ population (7, 44, 45). The GFRα1$^+$ population is comprised of mainly A_s and A_{pr} cells, whereas the Ngn3$^+$ population consists mainly of A_{al} cells. Axin2 expression does not discriminate between these possible subpopulations; the whole-mount immunostaining analysis of pulse-labeled Axin2$^{CreERT2/+}$; Rosa26$^{mTmG/+}$ testis revealed that the majority of Axin2$^+$ cells are PLZF$^+$ undifferentiated spermatogonia (Fig. 2 *D* and *H*), which likely includes both GFRα1$^+$ (Fig. 2 *C* and *F*) and Ngn3$^+$ subpopulations. However, it should be pointed out that the labeling efficiency of GFRα1$^+$ cells is only 0.6%, which is lower than the labeling efficiency of PLZF$^+$ cells (2.5%) (Fig. 2*J*). In contrast, the Axin2-LacZ signal is observed in 77.5% of

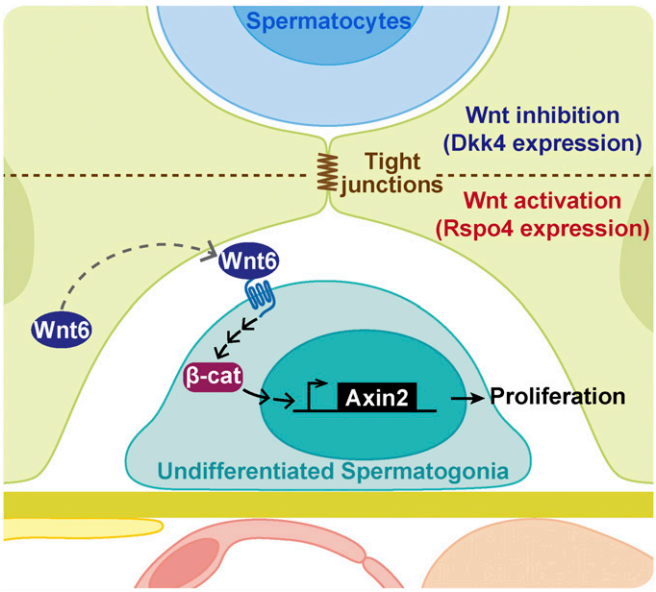

Fig. 7. Diagram summarizing cell–cell interactions between undifferentiated spermatogonia and Sertoli cells via Wnt/β-catenin signaling. Sertoli cells (green) provide a Wnt6 signal to activate Wnt/β-catenin signaling in undifferentiated spermatogonia (aqua). The latter cells express Wnt target genes, including *Axin2*, and subsequently proliferate. The tight junctions (brown) of Sertoli cells separate the basal compartment and the distribution of the Rspo4 protein from the Dkk4-enriched adluminal compartment.

GFRα1$^+$, higher than the percentage of LacZ$^+$ cells in the PLZF$^+$ populations (53.5%) (Fig. 1*E*). This slight difference between labeled populations may be a result of the differences in the time required for the detectable expression of the reporter genes.

We demonstrate that Axin2$^+$ undifferentiated spermatogonia contribute to spermatogenesis over the long term in the intact organ. In vivo genetic lineage tracing experiments using Axin2^{CreERT2} revealed that Axin2$^+$ undifferentiated spermatogonia meet the criteria of bona fide SSCs, as they self-renew and differentiate (Fig. 3 *B* and *C*). In several other organs, neutral competition/probabilistic stem cell fate models have been proposed in which adult stem cells are maintained as a pool with a flexible and dynamic character (31). In our study, multicolor lineage tracing revealed a pattern of decreasing clone number and increasing clone size over time (Fig. 4*C*). These data are consistent with previous studies that showing that SSCs follow a neutral competition model (6, 31, 33, 34), although additional, detailed analyses are needed to validate this model further.

This work highlights a particular role of Wnt/β-catenin signaling in the control of Axin2$^+$ undifferentiated spermatogonia in regulating the proliferation of PLZF$^+$ spermatogonia (Fig. 5*K*). This population contains both GFRα1$^+$ SSC-enriched subpopulations and progenitor-like subpopulations. Wnt/β-catenin signaling does not influence the maintenance of GFRα1$^+$ spermatogonia (Fig. 5*G*). Combined with the data from lineage-tracing analysis (Fig. 3*D*), these results raise the possibility that Wnt/β-catenin signaling is required for the generation of progenitor cells that are committed to differentiation from undifferentiated spermatogonia, whereas the maintenance of the stem cell pool via self-renewal is regulated by other mechanisms, such as GDNF (8) and Nanos2 (46). This finding agrees with in vitro experiments that indicate that Wnt/β-catenin signaling does not act primarily on SSCs but instead on progenitors (14). Although the majority of Axin2$^+$ cells are progenitors, it is not surprising that a portion of them are SSCs (Fig. 3*B*), in the light of a previous report that Ngn3$^+$ progenitors partly retain stem-like behavior (7). Interestingly, although Wnt/β-catenin signaling is known as a self-renewal signal for many adult tissue stem cells (9), in the context of adult testis homeostasis, Wnt promotes proliferation in SSCs/progenitor cells and may not have a critical role in maintaining SSC self-renewal.

A cautionary note, as with other β-catenin mutant experiments, is that β-catenin also plays a role in cadherin-mediated adherens junctions, complicating the interpretation of the genetic data (47) as well because E-cadherin expression is restricted to undifferentiated spermatogonia (48). We also note that mice mutant for β-catenin using other Cre drivers have phenotypes inconsistent with each other. In other studies, germ cell-specific β-catenin CKO mediated by Stra8-iCre, which is expressed in differentiating spermatogonia at the onset of differentiation, did not cause a detectable phenotype (49). In addition, spermatid-specific β-catenin CKO mediated by Prm1-Cre has been shown to cause impaired fertility as a result of reduced sperm counts (50). Another group reported disrupted spermatogenesis in both loss- and gain-of-Wnt signaling function experiments using AhCre (37). However, it is difficult to compare these phenotypes to those observed by us because of differences in target cell types or leaky Cre activity before induction. We suggest, therefore, that our approach is, to our knowledge, the first to highlight the function of Wnt/β-catenin signaling in undifferentiated spermatogonia.

Materials and Methods

Animals. Axin2^{CreERT2} mice were previously described (17). Axin2-lacZ mice were a gift from W. Birchmeier, Max Delbruck Center for Molecular Medicine, Berlin (51). Rosa26^{rbw} mice were a gift from I. L. Weissman, Stanford University School of Medicine, Stanford, CA (32). Rosa26^{mTmG} mice (26), β-catenin$^{\Delta ex2\text{-}6\text{-}fl}$ (35) mice, and Vasa-Cre mice (52) were obtained from The Jackson Laboratory. β-Catenin$^{\Delta ex2\text{-}6\text{-}del}$ mice, in which the β-catenin gene has been deleted ubiquitously, were generated by crossing β-catenin$^{\Delta ex2\text{-}6\text{-}fl}$ mice with Vasa-Cre mice. All experiments were approved by the Stanford University Animal Care and Use Committee and performed according to NIH guidelines.

X-Gal Staining. After the tunica albuginea was removed, the testes from 2-mo-old (P56) Axin2-lacZ mice were fixed for 10 min at room temperature in 4% (wt/vol) paraformaldehyde in PBS. Samples were washed in detergent rinse (PBS with 2 mM $MgCl_2$, 0.01% sodium deoxycholate, and 0.02% Nonidet P-40) and stained in staining solution (PBS with 2 mM $MgCl_2$, 0.01% sodium deoxycholate, 0.02% Nonidet P-40, 5 mM potassium ferricyanide, 5 mM potassium ferrocyanide, and 1 mg/mL X-gal) in the dark at room temperature overnight. Testes were then washed and postfixed overnight at 4 °C in 4% (wt/vol) paraformaldehyde. Paraffin-embedded X-gal–stained samples were sectioned and counterstained with nuclear fast red (Vector Laboratory) or immunostained with goat anti-GFRα1 (1:100; R&D Systems) or rabbit anti-PLZF antibody (1:100; Santa Cruz Biotechnology) using the Vectastain ABC system and NovaRED substrate kit (Vector Laboratory) according to the manufacturer's instructions.

Stereological Analysis. To assess the percentage of Axin2-LacZ$^+$ cells in GFRα1$^+$ and PLZF$^+$ undifferentiated spermatogonia, the testis sections of 2-mo-old Axin2-LacZ mice were analyzed using Stereo Investigator (MicroBrightField). GFRα1$^+$ and PLZF$^+$ cells from 200 and 100 images, respectively, were counted per mouse ($n = 3$) at a magnification of 400×. Fields were selected using a systematic uniform random sampling scheme.

Labeling and Lineage-Tracing Studies. Two-month-old (P56) mice received a single intraperitoneal injection of a 20-mg/mL stock solution of tamoxifen in corn oil/1% (vol/vol) ethanol, totaling 4-mg/20-g body weight, unless otherwise indicated. Control mice were injected with the filtered corn oil/ethanol vehicle only (data not shown). Mice were killed at various time points by carbon dioxide asphyxiation and cervical dislocation.

Immunostaining and Histology. The testes were fixed overnight in 4% (wt/vol) paraformaldehyde at 4 °C after the tunica albuginea was removed, immersed in sucrose gradients (10%, 20%, and 30% wt/vol) in PBS sequentially at 4 °C, then tissues were embedded in optimal cutting temperature compound (OCT). Frozen samples were sectioned at 8 μm using CryoJane (Leica Microsystems). Cryosections were incubated in blocking buffer [5% (vol/vol) Normal Donkey Serum, 0.02% Tween-20 in PBS] at room temperature and stained with primary and secondary antibodies, then mounted in Prolong Gold with DAPI mounting medium (Life Technologies). The primary antibodies used were chicken anti-GFP (1:1,000; Abcam), rabbit anti-PLZF (1:100; Santa Cruz), goat anti-GFRα1 (1:100; R&D Systems), goat anti-SCFR/cKit antibody (1:100; R&D Systems), rabbit anti-Sox9 (1:100; Millipore), and rat anti-Ki67 (1:200; eBioscience). For whole-mount immunostaining of seminiferous tubules, testes were fixed overnight in 4% (wt/vol) paraformaldehyde at 4 °C, then seminiferous tubules were untangled and separated from interstitial tissues using forceps. The seminiferous tubules were subjected to a regular immunostaining protocol, as described above. For H&E staining, the testes were fixed overnight in Bouin's solution (Sigma) at room temperature, dehydrated in a series of increasing alcohol concentrations, and embedded in paraffin. Paraffin sections (5 μm) were stained with Mayer's Hematoxylin, blued in a tap water, stained in Eosin solution, further dehydrated up to 100% ethanol, cleared in Orange Terpene, and then mounted with EcoMount (BioCare Medical).

RNA in Situ Hybridization. All in situ hybridization experiments were carried out with an RNAscope (53) on 2-mo-old (P56) wild-type mice. Testes were fixed in 10% (vol/vol) neutral buffered formalin at room temperature for 24 h, dehydrated, and embedded in paraffin. Tissue sections cut at 5-μm thickness were processed for RNA in situ detection using the RNAscope 2.0 High Definition-RED Kit or RNAscope 2-plex Detection Kit according to the manufacturer's instructions (ACDBio). Sequences of the probes used in the study are as follows: Wnt6 (NM_009526.3, 780–2026), Sox9 (NM_011448.4, 2157–3789), Dkk4 (NM_145592.2, 22–1140), and Rspo4 (NM_001040689.1, 1180–2202).

Microscopy and Imaging. Whole-mount images of X-gal stained seminiferous tubules were collected using the Zeiss Axioplan 2 imaging system. Bright-field images and immunofluorescence images of sectioned Axin2$^{CreERT2/+}$;Rosa26$^{mTmG/+}$ samples were collected using the Zeiss Axio Imager Z2 (Carl Zeiss). Fluorescent images of sectioned Axin2$^{CreERT2/+}$;Rosa26$^{rbw/+}$ were obtained using the Leica SP8 Confocal Microscope (Leica Microsystems). Whole-mount immunofluorescence images and immunofluorescence images of sectioned β-catenin CKO samples used for cell counting were obtained using the Zeiss Cell Observer Spinning

Disk Confocal Microscope. Tiling and image stitching were performed as appropriate using the Leica LAS AF system or Zeiss ZEN 2012 blue edition software. Pictures of newborn mice were taken using the Panasonic Lumix DMC-FX35 digital camera (Panasonic), with Zeiss fluorescence filter cubes (Filter set 38 HE, mGFP; Filter set 47, mCerulean; Filter set 43, mOrange; and Filter set 71, mCherry). Gross images of the testes were taken using the Leica M80.

Conditional Knockout of β-Catenin. Control Axin2$^{CreERT2/+}$;β-catenin$^{\Delta ex2\text{-}6\text{-}fl/+}$ and mutant Axin2$^{CreERT2/+}$;β-catenin$^{\Delta ex2\text{-}6\text{-}fl/del}$ animals were injected with three doses of tamoxifen corresponding to 3-mg/25-g body weight at 2 mo of age (P56) every other day. Testes were harvested and processed for histology and immunostaining after 5 wk of chase.

Statistical Analysis. All statistical analyses were performed using the Student's *t* test using GraphPad Prism. Results are presented as mean ± SEM. Statistical significance was set at $*P < 0.05$; $**P < 0.01$; $***P < 0.001$.

ACKNOWLEDGMENTS. We thank members of the H.M.T. and R.N. laboratories, especially M. Mizutani, C. Logan, and D. Zhao, for valuable input and discussions; I. Ajioka and M. Oshikawa for advice on stereology; S. H. Tan for critical reading of the manuscript; and Y. Kanai for technical advice on methodologies. This study was supported in part by the Japan Society for the Promotion of Science Research Fellowship for Young Scientists (to H.M.T.) and the Japan Society for the Promotion of Science Postdoctoral Fellowship for Research Abroad (to H.M.T.). R.N. is an Investigator of the Howard Hughes Medical Institute.

1. Johnson L, May MR, Busbee DL, Williams JD (1992) Effect of age and dietary restriction on daily sperm production and number and transit time of epididymal spermatozoa in the mouse. *Age (Omaha)* 15(3):65–71.
2. Krausz C (2011) Male infertility: Pathogenesis and clinical diagnosis. *Best Pract Res Clin Endocrinol Metab* 25(2):271–285.
3. Poongothai J, Gopenath TS, Manonayaki S (2009) Genetics of human male infertility. *Singapore Med J* 50(4):336–347.
4. Oatley JM, Brinster RL (2012) The germline stem cell niche unit in mammalian testes. *Physiol Rev* 92(2):577–595.
5. Oakberg EF (1971) Spermatogonial stem-cell renewal in the mouse. *Anat Rec* 169(3): 515–531.
6. Hara K, et al. (2014) Mouse spermatogenic stem cells continually interconvert between equipotent singly isolated and syncytial states. *Cell Stem Cell* 14(5):658–672.
7. Nakagawa T, Sharma M, Nabeshima Y, Braun RE, Yoshida S (2010) Functional hierarchy and reversibility within the murine spermatogenic stem cell compartment. *Science* 328(5974):62–67.
8. Meng X, et al. (2000) Regulation of cell fate decision of undifferentiated spermatogonia by GDNF. *Science* 287(5457):1489–1493.
9. Clevers H, Loh KM, Nusse R (2014) Stem cell signaling. An integral program for tissue renewal and regeneration: Wnt signaling and stem cell control. *Science* 346(6205): 1248012.
10. Jeays-Ward K, Dandonneau M, Swain A (2004) Wnt4 is required for proper male as well as female sexual development. *Dev Biol* 276(2):431–440.
11. Ohinata Y, et al. (2009) A signaling principle for the specification of the germ cell lineage in mice. *Cell* 137(3):571–584.
12. Parr BA, McMahon AP (1998) Sexually dimorphic development of the mammalian reproductive tract requires Wnt-7a. *Nature* 395(6703):707–710.
13. Yeh JR, Zhang X, Nagano MC (2011) Wnt5a is a cell-extrinsic factor that supports self-renewal of mouse spermatogonial stem cells. *J Cell Sci* 124(Pt 14):2357–2366.
14. Yeh JR, Zhang X, Nagano MC (2012) Indirect effects of Wnt3a/β-catenin signalling support mouse spermatogonial stem cells in vitro. *PLoS One* 7(6):e40002.
15. Golestaneh N, et al. (2009) Wnt signaling promotes proliferation and stemness regulation of spermatogonial stem/progenitor cells. *Reproduction* 138(1):151–162.
16. Jho E-H, et al. (2002) Wnt/β-catenin/Tcf signaling induces the transcription of Axin2, a negative regulator of the signaling pathway. *Mol Cell Biol* 22(4):1172–1183.
17. van Amerongen R, Bowman AN, Nusse R (2012) Developmental stage and time dictate the fate of Wnt/β-catenin-responsive stem cells in the mammary gland. *Cell Stem Cell* 11(3):387–400.
18. Lien W-H, et al. (2014) In vivo transcriptional governance of hair follicle stem cells by canonical Wnt regulators. *Nat Cell Biol* 16(2):179–190.
19. Volkenstein S, et al. (2013) Transient, afferent input-dependent, postnatal niche for neural progenitor cells in the cochlear nucleus. *Proc Natl Acad Sci USA* 110(35): 14456–14461.
20. Bowman AN, van Amerongen R, Palmer TD, Nusse R (2013) Lineage tracing with Axin2 reveals distinct developmental and adult populations of Wnt/β-catenin-responsive neural stem cells. *Proc Natl Acad Sci USA* 110(18):7324–7329.
21. Lim X, et al. (2013) Interfollicular epidermal stem cells self-renew via autocrine Wnt signaling. *Science* 342(6163):1226–1230.
22. Buageaw A, et al. (2005) GDNF family receptor alpha1 phenotype of spermatogonial stem cells in immature mouse testes. *Biol Reprod* 73(5):1011–1016.
23. Hofmann M-C, Braydich-Stolle L, Dym M (2005) Isolation of male germ-line stem cells; influence of GDNF. *Dev Biol* 279(1):114–124.
24. Buaas FW, et al. (2004) Plzf is required in adult male germ cells for stem cell self-renewal. *Nat Genet* 36(6):647–652.
25. Costoya JA, et al. (2004) Essential role of Plzf in maintenance of spermatogonial stem cells. *Nat Genet* 36(6):653–659.
26. Muzumdar MD, Tasic B, Miyamichi K, Li L, Luo L (2007) A global double-fluorescent Cre reporter mouse. *Genesis* 45(9):593–605.
27. Kluin PM, de Rooij DG (1981) A comparison between the morphology and cell kinetics of gonocytes and adult type undifferentiated spermatogonia in the mouse. *Int J Androl* 4(4):475–493.
28. Clermont Y, Trott M (1969) Duration of the cycle of the seminiferous epithelium in the mouse and hamster determined by means of 3H-thymidine and radioautography. *Fertil Steril* 20(5):805–817.
29. Russell LD, Sinha-Hikim AP, Ettlin RA, Clegg ED (1990) *Histological and Histopathological Evaluation of the Testis* (Cache River Press, Clearwater, FL).
30. Nakagawa T, Nabeshima Y, Yoshida S (2007) Functional identification of the actual and potential stem cell compartments in mouse spermatogenesis. *Dev Cell* 12(2): 195–206.
31. Klein AM, Simons BD (2011) Universal patterns of stem cell fate in cycling adult tissues. *Development* 138(15):3103–3111.
32. Ueno H, Weissman IL (2006) Clonal analysis of mouse development reveals a polyclonal origin for yolk sac blood islands. *Dev Cell* 11(4):519–533.
33. Klein AM, Nakagawa T, Ichikawa R, Yoshida S, Simons BD (2010) Mouse germ line stem cells undergo rapid and stochastic turnover. *Cell Stem Cell* 7(2):214–224.
34. Komai Y, et al. (2014) Bmi1 expression in long-term germ stem cells. *Sci Rep* 4:6175.
35. Brault V, et al. (2001) Inactivation of the beta-catenin gene by Wnt1-Cre-mediated deletion results in dramatic brain malformation and failure of craniofacial development. *Development* 128(8):1253–1264.
36. Cruciat C-M, Niehrs C (2013) Secreted and transmembrane wnt inhibitors and activators. *Cold Spring Harb Perspect Biol* 5(3):a015081.
37. Kerr GE, Young JC, Horvay K, Abud HE, Loveland KL (2014) Regulated Wnt/beta-catenin signaling sustains adult spermatogenesis in mice. *Biol Reprod* 90(1):3.
38. Namekawa SH, et al. (2006) Postmeiotic sex chromatin in the male germline of mice. *Curr Biol* 16(7):660–667.
39. Shima JE, McLean DJ, McCarrey JR, Griswold MD (2004) The murine testicular transcriptome: Characterizing gene expression in the testis during the progression of spermatogenesis. *Biol Reprod* 71(1):319–330.
40. Tan SH, et al. (2014) Wnts produced by Osterix-expressing osteolineage cells regulate their proliferation and differentiation. *Proc Natl Acad Sci USA* 111(49): E5262–E5271.
41. Wang B, Zhao L, Fish M, Logan CY, Nusse R (2015) Self-renewing diploid Axin2(+) cells fuel homeostatic renewal of the liver. *Nature* 524(7564):180–185.
42. Nair M, et al. (2008) Nuclear regulator Pygo2 controls spermiogenesis and histone H3 acetylation. *Dev Biol* 320(2):446–455.
43. Al Alam D, et al. (2011) Contrasting expression of canonical Wnt signaling reporters TOPGAL, BATGAL and Axin2(^{LacZ}) during murine lung development and repair. *PLoS One* 6(8):e23139.
44. Suzuki H, Sada A, Yoshida S, Saga Y (2009) The heterogeneity of spermatogonia is revealed by their topology and expression of marker proteins including the germ cell-specific proteins Nanos2 and Nanos3. *Dev Biol* 336(2):222–231.
45. Yoshida S (2012) Elucidating the identity and behavior of spermatogenic stem cells in the mouse testis. *Reproduction* 144(3):293–302.
46. Zhou Z, et al. (2015) RNA binding protein Nanos2 organizes post-transcriptional buffering system to retain primitive state of mouse spermatogonial stem cells. *Dev Cell* 34(1):96–107.
47. Nelson WJ, Nusse R (2004) Convergence of Wnt, beta-catenin, and cadherin pathways. *Science* 303(5663):1483–1487.
48. Tokuda M, Kadokawa Y, Kurahashi H, Marunouchi T (2007) CDH1 is a specific marker for undifferentiated spermatogonia in mouse testes. *Biol Reprod* 76(1): 130–141.
49. Rivas B, Huang Z, Agoulnik AI (2014) Normal fertility in male mice with deletion of β-catenin gene in germ cells. *Genesis* 52(4):328–332.
50. Chang Y-F, Lee-Chang JS, Harris KY, Sinha-Hikim AP, Rao MK (2011) Role of β-catenin in post-meiotic male germ cell differentiation. *PLoS One* 6(11):e28039.
51. Lustig B, et al. (2002) Negative feedback loop of Wnt signaling through upregulation of conductin/axin2 in colorectal and liver tumors. *Mol Cell Biol* 22(4):1184–1193.
52. Gallardo T, Shirley L, John GB, Castrillon DH (2007) Generation of a germ cell-specific mouse transgenic Cre line, Vasa-Cre. *Genesis* 45(6):413–417.
53. Wang F, et al. (2012) RNAscope: A novel in situ RNA analysis platform for formalin-fixed, paraffin-embedded tissues. *J Mol Diagn* 14(1):22–29.